 Communications in Theoretical Physics

Commun. Theor. Phys. **75** (2023) 105801 (9pp) https://doi.org/10.1088/1572-9494/acedfb

Security control of Markovian jump neural networks with stochastic sampling subject to false data injection attacks ⋆

Lan Yao[1], Xia Huang[1], Zhen Wang[1] and Min Xiao[2]

[1] College of Electrical Engineering and Automation, Shandong University of Science and Technology, Qingdao 266590, China
[2] College of Automation, Nanjing University of Posts and Telecommunications, Nanjing 210003, China

E-mail: huangxia_qd@126.com

Received 5 April 2023, revised 8 August 2023
Accepted for publication 8 August 2023
Published 13 September 2023

Abstract

The security control of Markovian jumping neural networks (MJNNs) is investigated under false data injection attacks that take place in the shared communication network. Stochastic sampled-data control is employed to research the exponential synchronization of MJNNs under false data injection attacks (FDIAs) since it can alleviate the impact of the FDIAs on the performance of the system by adjusting the sampling periods. A multi-delay error system model is established through the input-delay approach. To reduce the conservatism of the results, a sampling-period-probability-dependent looped Lyapunov functional is constructed. In light of some less conservative integral inequalities, a synchronization criterion is derived, and an algorithm is provided that can be solved for determining the controller gain. Finally, a numerical simulation is presented to confirm the efficiency of the proposed method.

Keywords: Markovian jumping neural networks, stochastic sampling, looped-functional, false data injection attack

(Some figures may appear in colour only in the online journal)

1. Introduction

The Markovian jump system (MJS) is a class of special switched systems, that can describe various emergencies that occur in industrial systems. An MJS has multiple working modes and it will switch among these modes based on a Markov chain. Because MJSs can reflect the characteristics of jump among different system modes, which greatly overcomes the limitations of a single system, it has great flexibility in simulating practical engineering systems. MJSs are widely used in satellite systems, image processing, security communications and other fields. Under this background and trend, the study of MJSs has important practical significance and practical value for modeling practical systems with finite modes. In the past decades, many outstanding achievements have been gained [1–3], including stability, synchronization, and filtering. In addition, chaotic synchronous communication is currently a hot research topic internationally [4, 5]. Markovian jumping neural networks (MJNNs) have broad application prospects in the fields of image encryption and audio encryption by utilizing the chaos synchronization of MJNNs, which has been widely discussed in [6–10].

With the ongoing advancements in digital control technology, sampled-data control (SDC) has gained extensive development in [9–14], which can effectively solve the problem of data redundancy. However, due to the openness of communication networks, SDC systems are vulnerable to malicious cyber attacks [15–17], which may degrade the system performance or even compromise the stability of the SDC system. Therefore, the security control problem of SDC systems has been widely discussed by researchers. There are many types of cyber attacks, mainly including deception

★ This work was supported by the NNSF of China under Grants 61973199, 62003794, 62173214, the Shandong Provincial NSF ZR2020QF050, ZR2021MF003.

attacks [18–21], DoS attacks [22], and false data injection attacks (FDIA) [23–25]. Therein, FDIA, as a common type of attack, can destroy the integrity of communication data by sending error information to the receiver, thus causing unpredictable damage to the SDC system. In [23], the security problem for the state estimation of the networked control system was discussed by proposing a specific algorithm of generating attacks to estimate the insecurity of the system. In [24], the stability of switched semi-MJSs was investigated under the FDIAs by using a reduced-order sliding mode control. Following this trend, it is a key issue to design appropriate mechanisms to alleviate the impact of attacks, which motivates our present research.

On the other hand, non-ideal network environments can bring about unpredictable network phenomena, such as time delay and sampling errors, which will inevitably lead to the jitter of the sampling period. To address this problem, the stochastic sampled-data control (SSDC) method has been proposed in [26]. SSDC allows the existence of multiple sampling periods with certain occurrence probability, that is, it allows the sampling period to jitter to a certain extent. Therefore, the SSDC can not only adjust the sampling period more flexibly to cope with the sampling error, but also alleviate the impact of cyber attacks on the performance of the controlled system. Hence, SSDC has attracted extensive attention [26–28]. Unfortunately, there are few works on the study of security control of MJNNs under FDIA via SSDC, which motivates the research of this article.

Recently, the looped Lyapunov functional (LLF) technique has been extensively employed for analyzing the stability of SDC systems [29–32]. Unlike the traditional Lyapunov functional, LLFs replace the positive definitiveness restriction with a loop condition. That is to say, the LLF relaxes the requirement for the functional to be positively definite in the sampling interval. Therefore, the conservatism of the obtained results can be relaxed by using the LLF method. In addition, LLF has the ability to fully utilize the state information of the sampled data system. However, the construction of LLFs for MJNNs subject to cyber attacks and stochastic sampling is difficult. Hence, the primary objective of this article is to develop an LLF and the corresponding analysis method for exponential synchronization of MJNNs via stochastic sampling.

Summarizing the aforementioned considerations, the security control of MJNNs under the FDIAs is investigated by using LLF, and the main contributions are threefold:

(1) To alleviate the impact of FDIA on the performance of the MJNNs, SSDC is developed to investigate the security control of the controlled system;
(2) The model of the error system with multi-delays is established. Associated with it, a sampling-period-probability-dependent LLF is constructed to reduce the conservatism of the main results.
(3) A less conservative exponential synchronization criterion and a design algorithm for determining the controller gain are given, respectively.

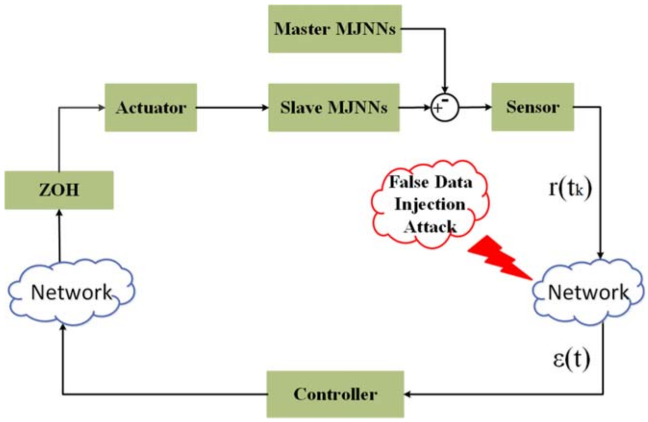

Figure 1. The structure of the secure control under FDIAs.

Notations: Denote $\mathbb{R}^n$ be the n-dimensional Euclidean space. Let $*$ and I_n (0_n) be the symmetric entries in a symmetric matrix and n-dimension identity (zero) matrix, respectively. Q^{T}, Q^{-1}, Sym$\{Q\}$ and $Q>0$ denote the transpose, inverse of matrix Q, $Q+Q^{\mathrm{T}}$ and the symmetric and positive definite matrix, respectively. diag$\{\cdots\}$ and col$\{\cdot\}$ denote the diagonal matrix and column vector. Prob$\{X\}$ and $\mathbb{E}\{\cdot\}$ denote the probability and the mathematical expectation of event, respectively. $\lambda_{\min}$ $(\lambda_{\max})$ and max$\{m, n\}$ refer to the maximum (minimum) eigenvalue and the largest value of m and n, respectively. $(\Omega, \mathcal{F}, \mathcal{P})$ represents the complete probability space.

2. Problem description

The schematic diagram of the security control of MJNNs under FDIAs occurred in the communication network channel is shown in figure 1. In figure 1, the sensor transmits the sampled data by stochastic sampling.

In figure 1, the time-varying delayed master-slave MJNNs can be described as:

$$\begin{cases}\dot{m}(t)=-C(\sigma(t))m(t)+A(\sigma(t))\chi(m(t))+B(\sigma(t))\chi(m(t-\tau(t))),\\ \dot{s}(t)=-C(\sigma(t))s(t)+A(\sigma(t))\chi(s(t))+B(\sigma(t))\chi(s(t-\tau(t)))+u(t),\end{cases}\tag{1}$$

where $m(t)$, $s(t)$, $u(t)\in\mathbb{R}^n$ are the state vectors of the master system, the slave system and the control input, respectively; $\chi(\cdot)\in\mathbb{R}^n$ is a nonlinear function satisfying $H_j^-\leqslant\frac{\chi_j(s_1)-\chi_j(s_2)}{s_1-s_2}\leqslant H_j^+$ and $\chi_j(0)=0$, where H_j^-, H_j^+ are constants; $\tau(t)$ denote a time delay with $0<\tau_1\leqslant\tau(t)\leqslant\tau_2$ and $\dot{\tau}(t)\leqslant\mu$, and τ_1, τ_2, μ are scalars. Denote $\sigma(t)$ as the Markov chain on $(\Omega, \mathcal{F}, \mathcal{P})$ with $\sigma(t)\in\mathcal{R}=\{1, 2,\ldots,\epsilon\}$ and $\Pi\triangleq\{\pi_{iq}\}_{\epsilon\times\epsilon}$ is the transition rate matrix:

$$\mathrm{Prob}\{\sigma(t+\delta_t)=q|\sigma(t)=i\}=\begin{cases}\pi_{iq}\delta_t+\mathrm{o}(\delta_t), & q\neq i,\\ 1+\pi_{ii}\delta_t+\mathrm{o}(\delta_t), & q=i,\end{cases}$$

where $\lim_{\delta_t\to 0}\frac{\mathrm{o}(\delta_t)}{\delta_t}=0$, $\pi_{iq}\geqslant 0\,(q\neq i)$ is the transition rate and $\pi_{ii} = -\sum_{q=1,q\neq i}^{\epsilon} \pi_{iq}$. Denote $C(\sigma(t)) \triangleq C_i$, $A(\sigma(t)) \triangleq A_i$ and $B(\sigma(t)) \triangleq B_i$ $(i \in \mathcal{R})$ are the system matrices.

Let $r(t) = s(t) - m(t)$ be the state error of the master and slave system, then the corresponding error system can be represented as:

$$\begin{aligned}\dot{r}(t) &= -C_i r(t) + A_i \varpi(r(t)) \\ &+ B_i \varpi(r(t-\tau(t))) + u(t),\end{aligned} \quad (2)$$

where $\varpi(r(t)) = \chi(s(t)) - \chi(m(t))$, $\varpi(r(t-\tau(t))) = \chi(s(t-\tau(t))) - \chi(m(t-\tau(t)))$ and

$$H_j^- \leqslant \frac{\varpi_j(s)}{s} \leqslant H_j^+, \; s \neq 0.$$

Assumption 1. Suppose there exist m sampling periods satisfying $0 = h^0 < h^1 < h^2 < \cdots < h^m$, and the occurrence probability of each sampling period is recognized as $\mathrm{Prob}\{h_k = h^j\} = \beta_j$, $j = 1, 2, \ldots, m$.
Obviously, $\sum_{j=1}^m \beta_j = 1$.

Represent the set of sampling instants as $\{t_k\}_{k\in\mathbb{N}}$. For $t \in [t_k, t_{k+1})$, the SSDC-based controller is designed:

$$u(t) = -K(s(t_k) - m(t_k)) = -Kr(t_k), \quad (3)$$

where K represents the gain matrix of the controller that requires designing later.

Define $d(t) \triangleq t - t_k$, then there are m cases for the location of $d(t)$. If the sampling period $h_k = h^j$, $j = 1, \ldots, m$, then we have

$$\begin{aligned}&\mathrm{Prob}\{0 \leqslant d(t) < h^1 | h_k = h^j\} = \tfrac{h^1}{h^j}, \\ &\mathrm{Prob}\{h^1 \leqslant d(t) < h^2 | h_k = h^j\} = \tfrac{h^2 - h^1}{h^j}, \\ &\cdots\cdots \\ &\mathrm{Prob}\{h^{j-1} \leqslant d(t) < h^j | h_k = h^j\} = \tfrac{h^j - h^{j-1}}{h^j}.\end{aligned}$$

Thus, the occurrence probability of the event $h^{j-1} \leqslant d(t) < h^j$, $j = 1, 2, \ldots, m$, can be calculated by using the law of total probability:

$$\begin{aligned}&\mathrm{Prob}\{0 \leqslant d(t) < h^1\} = \beta_1 + \beta_2 \tfrac{h^1}{h^2} + \cdots + \beta_m \tfrac{h^1}{h^m} \triangleq \gamma_1, \\ &\mathrm{Prob}\{h^1 \leqslant d(t) < h^2\} = \beta_2 \tfrac{h^2 - h^1}{h^2} + \cdots \\ &+ \beta_m \tfrac{h^2 - h^1}{h^m} \triangleq \gamma_2, \\ &\cdots\cdots \\ &\mathrm{Prob}\{h^{m-1} \leqslant d(t) < h^m\} = \beta_m \tfrac{h^m - h^{m-1}}{h^m} \triangleq \gamma_m.\end{aligned}$$

To quantify the above events, for $j = 1, \ldots, m$, total $2m$ random variables satisfying Bernoulli distribution introduce:

$$\beta_j(t) = \begin{cases} 1, & h_k = h^j, \\ 0, & \text{else}, \end{cases} \quad \gamma_j(t) = \begin{cases} 1, & h^{j-1} \leqslant d(t) < h^j, \\ 0, & \text{else}. \end{cases}$$

Then, we can calculate that

$$\begin{aligned}&\mathrm{Prob}\{\beta_j(t) = 1\} = \mathrm{Prob}\{h_k = h^j\} = \beta_j, \\ &\mathrm{Prob}\{\gamma_j(t) = 1\} = \mathrm{Prob}\{h^{j-1} \leqslant d(t) < h^j\} = \gamma_j.\end{aligned}$$

Furthermore, to specially describe the input delay $d(t)$ on intervals $[h^{j-1}, h^j)$, denote $d(t) \triangleq d_j(t)$ when $h^{j-1} \leqslant d(t) < h^j$. Then, the control input (3) that contains stochastic sampling can be modeled as follows:

$$u(t) = -Kr(t_k) = -\sum_{j=1}^m \gamma_j(t) Kr(t - d_j(t)). \quad (4)$$

Because the FDIAs occurred in the network channel randomly, the random attack can be described by introducing the random variable $\alpha(t)$:

$$\alpha(t) = \begin{cases} 1, & \text{attack is occurred}, \\ 0, & \text{else}. \end{cases}$$

Then, we have

$$\begin{aligned}&\mathrm{Prob}\{\alpha(t) = 1\} = \alpha, \; \mathrm{Prob}\{\alpha(t) = 0\} = 1 - \alpha, \\ &\mathbb{E}\{\alpha(t)\} = \alpha.\end{aligned}$$

In addition, due to the attack signal $g(t)$ is limited by the attack energy, Assumption 2 is needed.

Assumption 2. For $g(t)$, suppose there exists constant matrix G satisfying

$$\|g(t)\|^2 \leqslant \|Gr(t)\|^2$$

Then, the signal transmitted to the controller can be rewritten:

$$\varepsilon(t) = \sum_{j=1}^m \gamma_j(t) r(t - d_j(t)) + \alpha(t) g(t).$$

Thus, the control input under the FDIAs is expressed as

$$u(t) = -K\varepsilon(t) = -\sum_{j=1}^m \gamma_j(t) Kr(t - d_j(t)) - \alpha(t) Kg(t). \quad (5)$$

Combining (2) with (5), the closed-loop system (2) can be represented:

$$\begin{aligned}\dot{r}(t) &= -C_i r(t) + A_i \varpi(r(t)) + B_i \varpi(r(t-\tau(t))) \\ &- \sum_{j=1}^m \gamma_j(t) Kr(t - d_j(t)) - \alpha(t) Kg(t).\end{aligned} \quad (6)$$

Remark 1. Note that different from the deterministic SDC, SSDC has multiple sampling periods, which can reflect the inherent characteristics of the sampling error. Hence, the SSDC system can not only ensure the system achieves the desired performance in a nonideal environment, but also reduce the redundancy of communication transmission. In light of the characteristics of SSDC, the position of $d_j(t)$ can be described by introducing a series of random variables $\gamma_j(t)$, which follow the Bernoulli distribution.

Remark 2. In an unsatisfactory network environment, attackers tamper with the transmission data by launching FDIAs to destroy system performance. In view of the randomness of the cyber attack, the data transmitted to the controller can be given by $\varepsilon(t)$ with random variable $\alpha(t)$. Under the FDIAs, SSDC can alleviate the impact of the attacks on the performance of the controlled system by adjusting the occurrence probability of the sampling periods.

3. Main results

For simplicity, The following symbols will be utilized:

$$\begin{aligned}
&\tilde{e}_l = [0_{n\times(l-1)n},\ I_n,\ 0_{n\times(4-l)n}],\quad l = 1,2,3,4,\\
&\tilde{e}_\nu = [0_{n\times(\nu-1)n}, I_n, 0_{n\times(8+4m-\nu)n}],\\
&\nu = 1,2,\ldots 8 + 4m,\\
&\overline{\psi}(t) = \mathrm{col}\{r(t), r(t_k)\},\ \xi_j = \mathrm{col}\\
&\left\{r(t), r(t-h^j), \frac{1}{h^j}\int_{t-h^j}^{t} r(\theta)\mathrm{d}\theta, \vartheta_j(t)\right\},\\
&\vartheta_j(t) = \frac{2}{(h^j)^2}\\
&\times\int_{t-h^j}^{t}\int_{t-h^j}^{s} r(\theta)\mathrm{d}\theta\mathrm{d}s,\\
&\psi_\nu(t) = \mathrm{col}\{r(t), r(t-d_\nu(t))\},\ j = 1,\ldots,m,\\
&\varpi(r(t)),\quad \varpi(r(t-\tau(t))),\quad g(t),\quad \vartheta_1(t),\ldots,\ \vartheta_m(t)\},\\
&\zeta(t) = \mathrm{col}\{r(t), \dot{r}(t), r(t-h^1),\cdots,\\
&r(t-h^m), r(t-\tau(t)), r(t-\tau_1),\\
&r(t-\tau_2), r(t-d_1(t)),\cdots, r(t-d_m(t)),\\
&H_1 = \mathrm{diag}(H_1^-H_1^+, H_2^-H_2^+,\ldots,H_n^-H_n^+),\quad H_2\\
&=\mathrm{diag}\left(\frac{H_1^-+H_1^+}{2}, \frac{H_2^-+H_2^+}{2},\ldots,\frac{H_n^-+H_n^+}{2}\right).
\end{aligned}$$

Theorem 1. *For given scalars $\alpha > 0$, $\delta > 0$, $h^j > 0$, $\beta_j > 0$, and feedback gain* K, *the master-slave MJNNs (1) has achieved exponential synchronization subject to FDIAs if there exist matrices $P_i > 0$ $(i \in \mathcal{R})$, $Q_j > 0$, $R_j > 0$, $S_l > 0$, diagonal matrices $\Lambda_1 > 0$, $\Lambda_2 > 0$, and arbitrary matrices M_1, M_2, S_4, U_j, $\overline{V}_j$, X_j^1, X_j^2, W_j^l $(j = 1,\ldots,m,\ l = 1, 2, 3)$ with appropriate dimensions, the following LMIs hold:*

$$\begin{bmatrix}\Theta_i & \widetilde{\Psi}\\ * & \widehat{R}\end{bmatrix} < 0,\quad \begin{bmatrix}\Upsilon_i & \widetilde{\Psi}\\ * & \widehat{R}\end{bmatrix} < 0, \tag{7}$$

$$\Xi_1 = \begin{bmatrix}S_3 & S_4\\ * & S_3\end{bmatrix} > 0, \tag{8}$$

where $\Theta_i = \Delta_i + \mathrm{Sym}\{\Gamma_9^{\mathrm{T}}\Gamma_{10}\}$, $\Upsilon_i = \Theta_i + \Omega_i$, $\widetilde{\Psi} = [\sqrt{\beta_1 h^1}\Psi_1, \sqrt{\beta_2 h^2}\Psi_2,\cdots,\sqrt{\beta_m h^m}\Psi_m]$

$$\begin{aligned}
\Delta_i ={}& \mathrm{Sym}\{\tilde{e}_1^{\mathrm{T}}P_i\tilde{e}_2\} + \tilde{e}_1\left(\delta P_i + S_1 + \sum_{k=1}^{\epsilon}\pi_{ik}P_k\right)\tilde{e}_1\\
&- \eta_3\tilde{e}_{m+3}^{\mathrm{T}}S_1\tilde{e}_{m+3} + \tilde{e}_2^{\mathrm{T}}(\eta_1 S_2 + \eta_2 S_3)\tilde{e}_2 - \Gamma_2^{\mathrm{T}}S_2\Gamma_2\\
&- \Gamma_3^{\mathrm{T}}\Xi_1\Gamma_3 + \Gamma_7^{\mathrm{T}}\Xi_2\Gamma_7 + \Gamma_8^{\mathrm{T}}\Xi_3\Gamma_8\\
&+ \sum_{j=1}^{m}\beta_j(\varrho_j\tilde{e}_2^{\mathrm{T}}R_j\tilde{e}_2\\
&+ \mathrm{e}^{-\delta h^{j-1}}\tilde{e}_{j+1}^{\mathrm{T}}Q_j\tilde{e}_{j+1}\\
&- \mathrm{e}^{-\delta h^j}\tilde{e}_{j+2}^{\mathrm{T}}Q_j\tilde{e}_{j+2} + \Gamma_{1j}^{\mathrm{T}}\mathrm{Sym}\\
&\times\{W_j^1\Pi_1 + W_j^2\Pi_2 + W_j^3\Pi_3\}\Gamma_{1j})\\
&- \sum_{j=1}^{m}\sum_{\nu=1}^{j}\beta_j\frac{h^\nu - h^{\nu-1}}{h^j}(\mathrm{Sym}\{\Gamma_{4\nu}^{\mathrm{T}}U_j\tilde{e}_1\}\\
&+ \mathrm{Sym}\{\Gamma_{4\nu}^{\mathrm{T}}\overline{V}_j\tilde{e}_{5+m+\nu}\} - \Gamma_{5\nu}^{\mathrm{T}}X_j\Gamma_{5\nu}),\\
\Omega_i ={}& \sum_{j=1}^{m}\sum_{\nu=1}^{j}\beta_j(h^\nu - h^{\nu-1})\mathrm{Sym}\{\Gamma_6^{\mathrm{T}}X_j\Gamma_{5\nu}\\
&+ \Gamma_{4\nu}^{\mathrm{T}}U_j\tilde{e}_2 + \delta\Gamma_{4\nu}^{\mathrm{T}}(U_j\tilde{e}_1 + \overline{V}_j\tilde{e}_{5+m+\nu})\\
&+ \tilde{e}_2^{\mathrm{T}}(U_j\tilde{e}_1 + \overline{V}_j\tilde{e}_{5+m+\nu})\}\\
&+ \sum_{j=1}^{m}\sum_{\nu=1}^{j}\beta_j(h^\nu - h^{\nu-1})\delta\Gamma_{5\nu}^{\mathrm{T}}X_j\Gamma_{5\nu},
\end{aligned}$$

and $\widehat{R} = \mathrm{diag}\{\widetilde{R}_1, \widetilde{R}_2,\cdots,\widetilde{R}_m\}$, $\Pi_1 = \tilde{e}_1 - \tilde{e}_2$, $\Pi_2 = \tilde{e}_1 + \tilde{e}_2 - 2\tilde{e}_3$, $\Pi_3 = \tilde{e}_1 - \tilde{e}_2 - 6\tilde{e}_3 + 6\tilde{e}_4$, $\widetilde{R}_j = \mathrm{diag}\{-R_j, -3R_j, -5R_j\}$, $\Psi_j = [\Gamma_{1j}^{\mathrm{T}}W_j^1, \Gamma_{1j}^{\mathrm{T}}W_j^2, \Gamma_{1j}^{\mathrm{T}}W_j^3]$, $\Gamma_{1j} = \mathrm{col}\{\tilde{e}_1, \tilde{e}_{j+2}, \tilde{e}_{2(m+j)+7}, \tilde{e}_{2(m+j)+8}\}$, $\Gamma_2 = \tilde{e}_1 - \tilde{e}_{m+4}$, $\Gamma_3 = \mathrm{col}\{\tilde{e}_{m+4} - \tilde{e}_{m+3}, \tilde{e}_{m+3} - \tilde{e}_{m+5}\}$, $\Gamma_{4\nu} = \tilde{e}_1 - \tilde{e}_{5+m+\nu}$, $\Gamma_{5\nu} = \mathrm{col}\{\tilde{e}_1, \tilde{e}_{5+m+\nu}\}$, $\Gamma_6 = \mathrm{col}\{\tilde{e}_2, 0_{n\times n}\}$, $\Gamma_7 = \mathrm{col}\{\tilde{e}_1, \tilde{e}_{6+2m}\}$, $\Gamma_8 = \mathrm{col}\{\tilde{e}_1, \tilde{e}_{7+2m}\}$, $\Gamma_9 = M_1\tilde{e}_1 + M_2\tilde{e}_2$, $\Gamma_{10} = -\tilde{e}_2 - C_i\tilde{e}_1 + A_i\tilde{e}_{6+2m} + B_i\tilde{e}_{7+2m} - \sum_{j=1}^{m}\gamma_j K\tilde{e}_{5+m+j} - \alpha K\tilde{e}_{8+2m}$, $\varrho_j = \frac{1}{\delta}(\mathrm{e}^{\delta h^j} - \mathrm{e}^{\delta h^{j-1}})$, $\eta_1 = \frac{1}{\delta}\tau_1(\mathrm{e}^{\delta\tau_1} - 1)$, $\eta_2 = \frac{1}{\delta}(\tau_2 - \tau_1)(\mathrm{e}^{\delta\tau_2} - \mathrm{e}^{\delta\tau_1})$, $\eta_3 = (1-\mu)\mathrm{e}^{-\delta\tau_2}$, $\Xi_2 = \begin{bmatrix}-H_1\Lambda_1 & H_2\Lambda_1\\ * & -\Lambda_1\end{bmatrix}$, $\Xi_3 = \begin{bmatrix}-H_1\Lambda_2 & H_2\Lambda_2\\ * & -\Lambda_2\end{bmatrix}$.

Proof. The time-dependent LLF is constructed as follows:

$$\mathcal{W}(t) = \sum_{j=1}^{5} V_j(t),\quad t \in [t_k, t_{k+1}), \tag{9}$$

in which

$$\begin{aligned}
V_1(t) ={}& \mathrm{e}^{\delta t}r^{\mathrm{T}}(t)P(\sigma(t))r(t),\\
V_2(t) ={}& \sum_{j=1}^{m}\beta_j(t)\int_{t-h^j}^{t-h^{j-1}}\mathrm{e}^{\delta s}r^{\mathrm{T}}(s)Q_j r(s)\mathrm{d}s\\
&+ \sum_{j=1}^{m}\beta_j(t)\int_{-h^j}^{0}\int_{t+\theta}^{t}\mathrm{e}^{\delta(s-\theta)}\dot{r}^{\mathrm{T}}(s)R_j\dot{r}(s)\mathrm{d}s\mathrm{d}\theta,\\
V_3(t) ={}& \int_{t-\tau(t)}^{t}\mathrm{e}^{\delta s}r^{\mathrm{T}}(s)S_1 r(s)\mathrm{d}s\\
&+ \tau_1\int_{-\tau_1}^{0}\int_{t+\theta}^{t}\mathrm{e}^{\delta(s-\theta)}\dot{r}^{\mathrm{T}}(s)S_2\dot{r}(s)\mathrm{d}s\mathrm{d}\theta\\
&+ (\tau_2 - \tau_1)\int_{-\tau_2}^{-\tau_1}\int_{t+\theta}^{t}\mathrm{e}^{\delta(s-\theta)}\dot{r}^{\mathrm{T}}(s)S_3\dot{r}(s)\mathrm{d}s\mathrm{d}\theta,\\
V_4(t) ={}& 2\sum_{j=1}^{m}\beta_j(t)\mathrm{e}^{\delta t}(t_{k+1} - t)(r^{\mathrm{T}}(t)\\
&- r^{\mathrm{T}}(t_k))[U_j r(t) + \overline{V}_j r(t_k)],\\
V_5(t) ={}& \sum_{j=1}^{m}\beta_j(t)\mathrm{e}^{\delta t}(t_{k+1} - t)\overline{\psi}^{\mathrm{T}}(t)X_j\overline{\psi}(t),
\end{aligned}$$

where $X_j = \begin{bmatrix}\frac{\mathrm{Sym}\{X_j^1\}}{2} & -X_j^1 + X_j^2\\ * & -\mathrm{Sym}\{X_j^2\} + \frac{\mathrm{Sym}\{X_j^1\}}{2}\end{bmatrix}$.

For $V_4(t)$ and $V_5(t)$, through analyzing the characteristic of $(t_{k+1} - t)$-terms, $V_4(t)$ and $V_5(t)$ can be expressed with multi-delays as

$$\begin{aligned}
V_4(t) ={}& 2\sum_{j=1}^{m}\sum_{\nu=1}^{j}\beta_j(t)\gamma_\nu(t)\mathrm{e}^{\delta t}(h^j - d_\nu(t))\\
&\times(r^{\mathrm{T}}(t) - r^{\mathrm{T}}(t-d_\nu(t)))[U_j r(t) + \overline{V}_j r(t-d_\nu(t))],\\
V_5(t) ={}& \sum_{j=1}^{m}\sum_{\nu=1}^{j}\beta_j(t)\gamma_\nu(t)\mathrm{e}^{\delta t}(h^j - d_\nu(t))\psi_\nu^{\mathrm{T}}(t)X_j\psi_\nu(t).
\end{aligned}$$

Calculating $\mathcal{L}V_j(t)$ $(j = 1, 2,\ldots,5)$ along the trajectories of the error system (6), we have

$$\mathbb{E}\{\mathcal{L}V_1(t)\} = \mathbb{E}\{e^{\delta t}\zeta^{\mathrm{T}}(t)[\mathrm{Sym}\{\tilde{e}_1^{\mathrm{T}}P_i\tilde{e}_2\} + \tilde{e}_1\left(\delta P_i + \sum_{k=1}^{\epsilon}\pi_{ik}P_k\right)\tilde{e}_1\Bigg]\zeta(t)\Bigg\}. \tag{10}$$

For $V_2(t)$, we have

$$\begin{aligned}\mathbb{E}\{\mathcal{L}V_2(t)\} = \mathbb{E}\\ \Bigg\{\sum_{j=1}^{m}\beta_j(t)[&e^{\delta(t-h^{j-1})}r^{\mathrm{T}}(t-h^{j-1})Q_j r(t-h^{j-1})\\ &-e^{\delta(t-h^j)}r^{\mathrm{T}}(t-h^j)Q_j r(t-h^j)\\ &+e^{\delta t}\varrho_j\dot{r}^{\mathrm{T}}(t)R_j\dot{r}(t) - e^{\delta t}\int_{t-h^j}^{t}\dot{r}^{\mathrm{T}}(s)R_j\dot{r}(s)\mathrm{d}s\Bigg],\end{aligned}$$

where $\varrho_j = \frac{1}{\delta}(e^{\delta h^j} - e^{\delta h^{j-1}})$.

Combining with the less-conservative integral inequality [32], we have

$$-\mathbb{E}\left\{\int_{t-h^j}^{t}\dot{r}^{\mathrm{T}}(s)R_j\dot{r}(s)\mathrm{d}s\right\} \leqslant \mathbb{E}\{\xi_j^{\mathrm{T}}\Phi_j^1\xi_j\},$$

where $\Phi_j^1 = h^j(W_j^1R_j^{-1}(W_j^1)^{\mathrm{T}} + \frac{1}{3}W_j^2R_j^{-1}(W_j^2)^{\mathrm{T}} + \frac{1}{5}W_j^3R_j^{-1}(W_j^3)^{\mathrm{T}}) + \mathrm{Sym}\{W_j^1\Pi_1 + W_j^2\Pi_2 + W_j^3\Pi_3\}$.

Then, combining the above inequality, we have

$$\begin{aligned}\mathbb{E}\{\mathcal{L}V_2(t)\} \leqslant \mathbb{E}\Bigg\{\sum_{j=1}^{m}\beta_j(t)\\ \times[e^{\delta(t-h^{j-1})}r^{\mathrm{T}}(t-h^{j-1})Q_j r(t-h^{j-1})\\ -e^{\delta(t-h^j)}r^{\mathrm{T}}(t-h^j)Q_j r(t-h^j) + e^{\delta t}\varrho_j\dot{r}^{\mathrm{T}}(t)R_j\dot{r}(t)\\ -e^{\delta t}\xi_j^{\mathrm{T}}\Phi_j^1\xi_j].\end{aligned} \tag{11}$$

Thus, from (11), $\mathbb{E}\{\mathcal{L}V_2(t)\}$ can be estimated as:

$$\begin{aligned}\mathbb{E}\{\mathcal{L}V_2(t)\} \leqslant \mathbb{E}\Bigg\{\sum_{j=1}^{m}e^{\delta t}\beta_j\zeta^{\mathrm{T}}(t)\\ \times[\varrho_j\tilde{e}_2^{\mathrm{T}}R_j\tilde{e}_2 + e^{\delta\times(t-h^{j-1})}\tilde{e}_{j+1}^{\mathrm{T}}Q_j\tilde{e}_{j+1}\\ +\Gamma_{1j}^{\mathrm{T}}\Phi_j^1\Gamma_{1j}e^{-\delta h^j}\tilde{e}_{j+2}^{\mathrm{T}}Q_j\tilde{e}_{j+2}]\zeta(t)\}.\end{aligned}$$

For $V_3(t)$, the $\mathcal{L}V_3(t)$ can be calculated as:

$$\begin{aligned}\mathbb{E}\{\mathcal{L}V_3(t)\} \leqslant \mathbb{E}\{&e^{\delta t}[r^{\mathrm{T}}(t)S_1r(t) - e^{-\delta\tau(t)}(1-\mu)r^{\mathrm{T}}\\ &\times(t-\tau(t))S_1r(t-\tau(t))] + e^{\delta t}\dot{r}^{\mathrm{T}}(t)(\eta_1S_2\\ &+\eta_2S_3)\dot{r}(t) - e^{\delta t}\tau_1\int_{t-\tau_1}^{t}\dot{r}^{\mathrm{T}}(s)S_2\dot{r}(s)\mathrm{d}s\\ &-e^{\delta t}(\tau_2-\tau_1)\int_{t-\tau_2}^{t-\tau_1}\dot{r}^{\mathrm{T}}(s)S_3\dot{r}(s)\mathrm{d}s\Bigg\},\end{aligned}$$

where $\eta_1 = \frac{1}{\delta}\tau_1(e^{\delta\tau_1} - 1)$, $\eta_2 = \frac{1}{\delta}(\tau_2 - \tau_1)(e^{\delta\tau_2} - e^{\delta\tau_1})$.

According to the Jensen's inequality [33], the first integral term in $\mathcal{L}V_3(t)$ is estimated:

$$\begin{aligned}\mathbb{E}\left\{-\tau_1\int_{t-\tau_1}^{t}\dot{r}^{\mathrm{T}}(s)S_2\dot{r}(s)\mathrm{d}s\right\} \leqslant \mathbb{E}\\ \times\{-(r(t) - r(t-\tau_1))^{\mathrm{T}}S_2(r(t) - r(t-\tau_1))\}.\end{aligned}$$

Combining with the Jensen's inequality and the reciprocally convex inequality [34], the second integral term in $\mathcal{L}V_3(t)$ is estimated:

$$\begin{aligned}&\mathbb{E}\left\{-(\tau_2-\tau_1)\int_{t-\tau_2}^{t-\tau_1}\dot{r}^{\mathrm{T}}(s)S_3\dot{r}(s)\mathrm{d}s\right\}\\ &\leqslant\mathbb{E}\left\{-\phi^{\mathrm{T}}(t)\begin{bmatrix}S_3 & S_4\\ * & S_3\end{bmatrix}\phi(t)\right\},\end{aligned}$$

where $\phi(t) = \mathrm{col}\{r(t-\tau_1) - r(t-\tau(t)), r(t-\tau(t)) - r(t-\tau_2)\}$.

Thus, $\mathcal{L}V_3(t)$ can be estimated as

$$\begin{aligned}\mathbb{E}\{\mathcal{L}V_3(t)\} \leqslant \mathbb{E}\{&e^{\delta t}\zeta^{\mathrm{T}}(t)[\tilde{e}_1^{\mathrm{T}}S_1\tilde{e}_1 - \eta_3\tilde{e}_{m+3}^{\mathrm{T}}S_1\tilde{e}_{m+3}\\ &+\tilde{e}_2^{\mathrm{T}}(\eta_1S_2 + \eta_2S_3)\tilde{e}_2 - \Gamma_2^{\mathrm{T}}S_2\Gamma_2 - \Gamma_3^{\mathrm{T}}\Xi_1\Gamma_3]\zeta(t)\},\end{aligned}$$

where $\eta_3 = (1-\mu)e^{-\delta\tau_2}$.

For $V_4(t)$, we have

$$\begin{aligned}\mathbb{E}\{\mathcal{L}V_4(t)\} = \mathbb{E}\\ \Bigg\{2\sum_{j=1}^{m}\sum_{\nu=1}^{j}&\beta_j(t)\gamma_\nu(t)e^{\delta t}[\delta(h^j - d_\nu(t)) - 1](r^{\mathrm{T}}(t)\\ &-r^{\mathrm{T}}(t-d_\nu(t)))[U_jr(t) + \overline{V}_jr(t-d_\nu(t))]\\ &+2\sum_{j=1}^{m}\sum_{\nu=1}^{j}\beta_j(t)\gamma_\nu(t)e^{\delta t}(h^j - d_\nu(t))[\dot{r}^{\mathrm{T}}(t)[U_jr(t)\\ &+\overline{V}_jr(t-d_\nu(t))] + (r^{\mathrm{T}}(t) - r^{\mathrm{T}}(t-d_\nu(t)))U_j\dot{r}(t)]\Bigg\}.\end{aligned}$$

According to $\mathbb{E}\{\beta_j(t)\gamma_\nu(t)\} = \beta_j\frac{h^\nu - h^{\nu-1}}{h^j}$, we have

$$\begin{aligned}\mathbb{E}\{\mathcal{L}V_4(t)\} = \mathbb{E}\\ \Bigg\{2\sum_{j=1}^{m}\sum_{\nu=1}^{j}&e^{\delta t}\beta_j\frac{h^\nu - h^{\nu-1}}{h^j}[\delta(h^j - d_\nu(t)) - 1]\\ &\times(r^{\mathrm{T}}(t) - r^{\mathrm{T}}(t-d_\nu(t)))[U_jr(t)\\ &+\overline{V}_jr(t-d_\nu(t))] + 2\sum_{j=1}^{m}\sum_{\nu=1}^{j}e^{\delta t}\beta_j\frac{h^\nu - h^{\nu-1}}{h^j}(h^j - d_\nu(t))\\ &\times[\dot{r}^{\mathrm{T}}(t)U_jr(t) + \dot{r}^{\mathrm{T}}(t)\overline{V}_jr(t-d_\nu(t))\\ &+r^{\mathrm{T}}(t)U_j\dot{r}(t) - r^{\mathrm{T}}(t-d_\nu(t))U_j\dot{r}(t)]\Bigg\}.\end{aligned}$$

Then, we have

$$\begin{aligned}\mathbb{E}\{\mathcal{L}V_4(t)\} = \mathbb{E}\Bigg\{\sum_{j=1}^{m}\sum_{\nu=1}^{j}2e^{\delta t}\beta_j\frac{h^\nu - h^{\nu-1}}{h^j}\zeta^{\mathrm{T}}(t)\\ \times\{[\delta(h^j - d_\nu(t)) - 1]\Gamma_{4\nu}^{\mathrm{T}}[U_j\tilde{e}_1 + \overline{V}_j\tilde{e}_{5+m+\nu}]\\ +(h^j - d_\nu(t))[\tilde{e}_2^{\mathrm{T}}(U_j\tilde{e}_1 + \overline{V}_j\tilde{e}_{5+m+\nu}) + \Gamma_{4\nu}^{\mathrm{T}}U_j\tilde{e}_2]\}\zeta(t)\}.\end{aligned}$$

For $V_5(t)$, we have

$$\begin{aligned}\mathbb{E}\{\mathcal{L}V_5(t)\} = \mathbb{E}\Bigg\{\sum_{j=1}^{m}\sum_{\nu=1}^{j}\beta_j(t)\gamma_\nu(t)e^{\delta t}\{[\delta(h^j - d_\nu(t)) - 1]\\ \psi_\nu^{\mathrm{T}}(t)X_j\psi_\nu(t) + 2(h^j - d_\nu(t))\dot{\psi}_\nu^{\mathrm{T}}(t)X_j\psi_\nu(t)\}.\end{aligned}$$

Combining with $\mathbb{E}\{\beta_j(t)\gamma_\nu(t)\} = \beta_j \frac{h^\nu - h^{\nu-1}}{h^j}$, we have

$$\begin{aligned}\mathbb{E}\{\mathcal{L}V_5(t)\} = \mathbb{E}\Bigg\{& e^{\delta t}\sum_{j=1}^{m}\sum_{\nu=1}^{j}\beta_j \frac{h^\nu - h^{\nu-1}}{h^j}\zeta^{\mathrm{T}}(t)\\ &\{[\delta(h^j - d_\nu(t)) - 1]\Gamma_{5\nu}^{\mathrm{T}}X_j\Gamma_{5\nu}\\ &+2(h^j - d_\nu(t))\Gamma_6^{\mathrm{T}}(t)X_j\Gamma_{5\nu}\}\zeta(t)\Bigg\}. \end{aligned} \tag{12}$$

For the activation function $\varpi_j(\cdot)$, the following two inequalities hold:

$$\mathbb{E}\{(\varpi_j(r_j(t)) - H_j^- r_j(t)) \times (\varpi_j(r_j(t)) - H_j^+ r_j(t))\} \leqslant 0,$$

and

$$\begin{aligned}&\mathbb{E}\{(\varpi_j(r_j(t - \tau_j(t))) - H_j^- r_j(t - \tau_j(t)))\\ &\quad\times(\varpi_j(r_j(t - \tau_j(t))) - H_j^+ r_j(t - \tau_j(t)))\} \leqslant 0,\end{aligned}$$

this means that for $\Lambda_1 > 0$ and $\Lambda_2 > 0$, the two inequalities hold:

$$\mathbb{E}\left\{\begin{bmatrix} r(t) \\ \varpi(r(t)) \end{bmatrix}^{\mathrm{T}}\begin{bmatrix} -H_1\Lambda_1 & H_2\Lambda_1 \\ * & -\Lambda_1 \end{bmatrix}\begin{bmatrix} r(t) \\ \varpi(r(t)) \end{bmatrix}\right\} \geqslant 0, \tag{13}$$

and

$$\begin{aligned}\mathbb{E}\Bigg\{&\begin{bmatrix} r(t-\tau(t)) \\ \varpi(r(t-\tau(t))) \end{bmatrix}^{\mathrm{T}}\begin{bmatrix} -H_1\Lambda_2 & H_2\Lambda_2 \\ * & -\Lambda_2 \end{bmatrix}\\ &\times\begin{bmatrix} r(t-\tau(t)) \\ \varpi(r(t-\tau(t))) \end{bmatrix}\Bigg\}\geqslant 0,\end{aligned} \tag{14}$$

The inequalities (13) and (14) are equivalent to

$$\mathbb{E}\{\zeta^{\mathrm{T}}(t)\Gamma_7^{\mathrm{T}}\Xi_2\Gamma_7\zeta(t)\} \geqslant 0, \tag{15}$$

and

$$\mathbb{E}\{\zeta^{\mathrm{T}}(t)\Gamma_8^{\mathrm{T}}\Xi_3\Gamma_8\zeta(t)\} \geqslant 0. \tag{16}$$

Additionally, combining with the error system (6), for matrices M_1, M_2, the following equation holds:

$$\begin{aligned}0 = \mathbb{E}\Bigg\{&2e^{\delta t}[r^{\mathrm{T}}(t)M_1^{\mathrm{T}} + \dot{r}^{\mathrm{T}}(t)M_2^{\mathrm{T}}] \times [-\dot{r}(t) - C_i r(t)\\ &+ A_i\varpi(r(t)) + B_i\varpi(r(t-\tau(t)))\\ &- \sum_{j=1}^{m}\gamma_j(t)Kr(t - d_j(t)) - \alpha(t)Kg(t)]\Bigg\}.\end{aligned}$$

This is equivalent to

$$\mathbb{E}\{e^{\delta t}\zeta^{\mathrm{T}}(t)\mathrm{Sym}\{\Gamma_9^{\mathrm{T}}\Gamma_{10}\}\zeta(t)\} = 0. \tag{17}$$

Then, for $t \in [t_k, t_{k+1})$, $i \in \mathcal{R}$, combining inequalities (10)–(17), we obtain that

$$\begin{aligned}\mathbb{E}\{\mathcal{L}\mathcal{W}(t)\} \leqslant \mathbb{E}\Bigg\{&e^{\delta t}\zeta^{\mathrm{T}}(t)\Bigg(\frac{t_{k+1}-t}{t_{k+1}-t_k}\Upsilon_i\\ &+\frac{t-t_k}{t_{k+1}-t_k}\Theta_i + \sum_{j=1}^{m}\beta_j\Gamma_{1j}^{\mathrm{T}}\Phi_j^2\Gamma_{1j}\Bigg)\zeta(t)\Bigg\},\end{aligned} \tag{18}$$

where $\Phi_j^2 = h^j(W_j^1R_j^{-1}(W_j^1)^{\mathrm{T}} + \frac{1}{3}W_j^2R_j^{-1}(W_j^2)^{\mathrm{T}} + \frac{1}{5}W_j^3R_j^{-1}(W_j^3)^{\mathrm{T}})$.

From the LMIs (8)–(9), we have $\mathbb{E}\{\mathcal{L}\mathcal{W}(t)\} < 0$. Combining with the continuity of $\mathcal{W}(t)$ and $\mathbb{E}\{\mathcal{L}\mathcal{W}(t)\} < 0$, we have

$$\mathbb{E}\{\mathcal{W}(t_k)\} \leqslant \mathbb{E}\{\mathcal{W}(t_0)\}. \tag{19}$$

Integrating the error system (6) from t_k to t, we have

$$\begin{aligned}r(t) = r(t_k) &- \int_{t_k}^{t} C_i r(s)\mathrm{d}s + \int_{t_k}^{t} A_i\varpi(r(s))\mathrm{d}s\\ &+\int_{t_k}^{t} B_i\varpi(r(s-\tau(s)))\mathrm{d}s - \int_{t_k}^{t} Kr(t_k)\mathrm{d}s\\ &-\int_{t_k}^{t} \alpha(s)Kg(s)\mathrm{d}s.\end{aligned} \tag{20}$$

Combining with the Cauchy–Schwarz inequality [35], denote $\widehat{H} = \mathrm{diag}\{\max\{H_1^-, H_1^+\}, \max\{H_2^-, H_2^+\}, \cdots, \max\{H_n^-, H_n^+\}\}$, we have $\|A_i\varpi(r(t))\|^2 \leqslant \|A_i\|^2\|\widehat{H}\|^2\|r(t)\|^2$ and $\|B_i\varpi(r(t-\tau(t)))\|^2 \leqslant \|B_i\|^2\|\widehat{H}\|^2\|r(t-\tau(t))\|^2$, then

$$\begin{aligned}\mathbb{E}\{\|r(t)\|^2\} \leqslant \mathbb{E}\Bigg\{&6(1 + (h^m\|K\|)^2)\|r(t_k)\|^2\\ &+6h^m(\|C\|^2 + \|A\|^2\|\widehat{H}\|^2)\int_{t_k}^{t}\|r(s)\|^2\mathrm{d}s\\ &+6h^m\|B\|^2\|\widehat{H}\|^2\int_{t_k}^{t}\|r(s-\tau(s))\|^2\mathrm{d}s\Bigg\},\end{aligned}$$

where $\|C\|^2 = \max_{i\in\mathcal{R}}\{\|C_i\|^2\}$, $\|A\|^2 = \max_{i\in\mathcal{R}}\{\|A_i\|^2\}$, $\|B\|^2 = \max_{i\in\mathcal{R}}\{\|B_i\|^2\}$.

Thus, combining with the Gronwall-Bellman inequality [36], we can conclude

$$\mathbb{E}\{\|r(t)\|^2\} \leqslant \mathbb{E}\{\theta\|r(t_k)\|^2\}, \tag{21}$$

where $\theta = 6(1 + (h^m\|K\|)^2)e^{6(h^m\|C\|)^2 + 6(h^m(\|A\|+\|B\|)\|\widehat{H}\|)^2 + 6(h^m\|K\|\|G\|)^2}$.

Furthermore, based on the inequalities (13)–(14), we obtain

$$\begin{aligned}\mathbb{E}\{\|r(t)\|^2\} &\leqslant \mathbb{E}\{\theta\|r(t_k)\|^2\} = \mathbb{E}\left\{\frac{\eta\lambda_{\min}(P_i)e^{\delta t_k}}{\lambda_{\min}(P_i)e^{\delta t_k}}\|r(t_k)\|^2\right\}\\ &\leqslant\mathbb{E}\left\{\frac{\theta e^{\delta t_k}}{\lambda_{\min}(P_i)e^{\delta t_k}}r^{\mathrm{T}}(t_k)P_i r(t_k)\right\}\\ &\leqslant\mathbb{E}\left\{\frac{\theta}{\lambda_{\min}(P_i)e^{\delta t_k}}V_1(t_k)\right\}\\ &\leqslant\mathbb{E}\left\{\frac{\theta e^{\delta h^m}e^{-\delta t}}{\lambda_{\min}(P_i)}\mathcal{W}(t_k)\right\} \leqslant \mathbb{E}\left\{\frac{\theta e^{\delta h^m}e^{-\delta t}}{\lambda_{\min}(P_i)}\mathcal{W}(t_0)\right\}.\end{aligned} \tag{22}$$

From the inequality given above, we can conclude

$$\mathbb{E}\{\|r(t)\|^2\} \leqslant \omega e^{-\delta t}\mathbb{E}\{\|r(t_0)\|_c^2\},$$

where

$\omega = \varrho\frac{\theta e^{\delta h^m}}{\lambda_{\min}(P_i)} > 0$,

$\varrho = \lambda_{\max}(P_i) + \tau_2\lambda_{\max}(S_1) + \frac{\tau_1^3}{2}\lambda_{\max}(S_2) + \frac{(\tau_2-\tau_1)^3}{2}\lambda_{\max}(S_3)$.

Hence, the master-slave MJNNs (1) achieve exponential synchronization via controller (5) under FDIAs. That completes the proof.

Remark 3. In this paper, the time-dependent looped-functional $\mathcal{W}(t)$ is constructed. From $\mathcal{W}(t)$, we can easily see that the positive definiteness of the functional matrices U_j, $\overline{V}_j$, X_j are not required. That is, $\mathcal{W}(t)$ relaxes the positive definite constraint of $\mathcal{W}(t)$ in the sampling interval, and only requires its positive definiteness at the sampling instants $\{t_k\}$, it contributes to relaxing the conservativeness of the stability

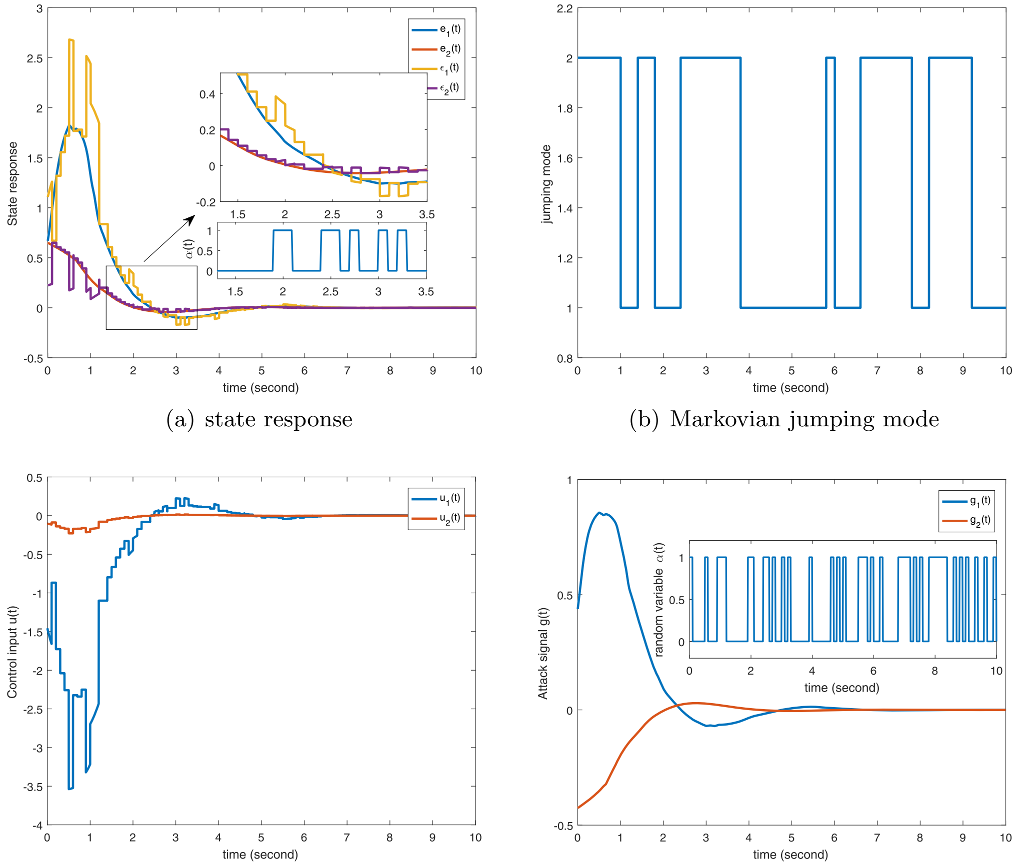

(a) state response (b) Markovian jumping mode

(c) control input (d) attack signal

Figure 2. (a) The time response of $r(t)$ and $\varepsilon(t)$; (b) Markov jumping mode; (c) the control input; (d) the attack signal $g(x(t))$ and $\alpha(t)$.

conditions and to increasing the maximum allowable bound of the sampling intervals.

Theorem 2. *For given constants $\alpha > 0$, $\delta > 0$, $h^j > 0$, $\beta_j > 0$, λ, in mean square sense, the master-slave MJNNs (1) has achieved exponential synchronization subject to FDIAs if there exist matrices $P_i > 0\ (i \in \mathcal{R})$, $Q_j > 0$, $R_j > 0$, $S_l > 0$, diagonal matrices $\Lambda_1 > 0$, $\Lambda_2 > 0$, and arbitrary matrices M_1, $\widetilde{K}$, S_4, U_j, $\overline{V}_j$, X_j^1, X_j^2, $W_j^l\ (j = 1, \ldots, m,\ l = 1, 2, 3)$ with appropriate dimensions, the following LMIs hold:*

$$\begin{bmatrix} \widetilde{\Theta}_i & \widetilde{\Psi} \\ * & \widehat{R} \end{bmatrix} < 0, \quad \begin{bmatrix} \widetilde{\Upsilon}_i & \widetilde{\Psi} \\ * & \widehat{R} \end{bmatrix} < 0, \quad \Xi_1 = \begin{bmatrix} S_3 & S_4 \\ * & S_3 \end{bmatrix} > 0, \tag{23}$$

where $\widetilde{\Theta}_i = \Delta_i + \mathrm{Sym}\{\Gamma_{11}^{\mathrm{T}}\Gamma_{12} + \Gamma_{13}^{\mathrm{T}}\Gamma_{14}\}$, $\widetilde{\Upsilon}_i = \widetilde{\Theta}_i + \Omega_i$, $\Gamma_{11} = M_1\tilde{e}_1 + \lambda M_1\tilde{e}_2$, $\Gamma_{12} = -\tilde{e}_2 - C_i\tilde{e}_1 + A_i\tilde{e}_{6+2m} + B_i\tilde{e}_{7+2m}$, $\Gamma_{13} = \tilde{e}_1 + \lambda\tilde{e}_2$, $\Gamma_{14} = -\sum_{j=1}^{m}\gamma_j\widetilde{K}\tilde{e}_{5+m+j} - \alpha\widetilde{K}\tilde{e}_{8+2m}$, and the blocks not mentioned earlier are defined identically to those in theorem 1. Then, the controller gain K *is given as $K = (M_1^{\mathrm{T}})^{-1}\widetilde{K}$.*

Proof. In view of the LMIs (7)–(8), we denote $M_2 = \lambda M_1$ and $\widetilde{K} = M_1^{\mathrm{T}}K$. The controller gain K can be calculated by $(M_1^{\mathrm{T}})^{-1}\widetilde{K}$ via employing the MATLAB/LMI Toolbox. That completes the proof.

Table 1. The maximum value of h^2 for different h^1 with $\beta_1 = 0.6$, $\beta_2 = 0.4$, $\delta = 0.5$.

h^1	0.01	0.05	0.1	0.15	0.2
$h^2_{\max}$ with $\alpha = 0.2$	0.834	0.786	0.682	0.533	0.363
$h^2_{\max}$ with $\alpha = 0.5$	0.457	0.426	0.357	0.258	

Remark 4. Significantly, the $\beta_j(t)$-dependent LLF $\mathcal{W}(t)$ contains the information of occurrence probability β_j for different sampling periods, thus, the derived synchronization conditions are β_j-dependent. When facing cyber attacks, we can adjust β_j to obtain an appropriate control gain K.

4. Numerical example

Consider the system parameters of a MJNN proposed in [6] as follows: $C_1 = \mathrm{diag}\{1,\ 0.9\}$, $C_2 = \mathrm{diag}\{1,\ 1\}$, $\pi_{12} = 0.5$,

Table 2. The maximum value of h^2 for different β_1 with $\delta = 0.1$, $h^1 = 0.1$.

β_1	0.1	0.2	0.3	0.4	0.5	0.6	0.7	0.8
$h^2_{\max}$	0.304	0.330	0.367	0.420	0.509	0.682	1.113	2.637

$\pi_{21} = 0.8$, $\chi(s) = \frac{|s+1| - |s-1|}{5}$, and

$$A_1 = \begin{bmatrix} 0.9 + \frac{\pi}{4} & 19 \\ 0.11 & 0.9 + \frac{\pi}{4} \end{bmatrix}, \quad A_2 = \begin{bmatrix} 1 + \frac{\pi}{4} & 19 \\ 0.09 & 1 + \frac{\pi}{4} \end{bmatrix},$$

$$B_1 = \begin{bmatrix} \frac{-1.2\sqrt{2}\pi}{4} & 0.3 \\ 0.2 & \frac{-1.2\sqrt{2}\pi}{4} \end{bmatrix},$$

$$B_2 = \begin{bmatrix} \frac{-1.3\sqrt{2}\pi}{4} & 0.1 \\ 0.1 & \frac{-1.3\sqrt{2}\pi}{4} \end{bmatrix}.$$

We can calculate $H_1 = \mathrm{diag}\{0, 0\}$ and $H_2 = \mathrm{diag}\{0.2, 0.2\}$. Take $\tau(t) = \frac{e^t}{1+e^t}$ with $\tau_1 = 0.5$, $\tau_2 = 1$, $\mu = 0.25$ and $g(t) = \tan(0.7r(t))$. The initial values are selected as $m(\theta) = [-0.4, -0.35]^{\mathrm{T}}$ and $s(\theta) = [0.27, 0.30]^{\mathrm{T}}$, $\theta \in [-1, 0]$.

According to theorem 1, tables 1 and 2 give the quantitative relationship between the occurrence probability β_1, the sampling periods h^1, h^2 and the attack probability α with $K = \begin{bmatrix} 1.6200 & -0.0022 \\ 0.1153 & 0.0734 \end{bmatrix}$.

Table 1 gives the maximum bound of h^2 for different h^1 and α with $\beta_1 = 0.6$, $\beta_2 = 0.4$, $\delta = 0.5$. From table 1, it is easy to see that the maximum value of h^2 becomes larger gradually with the decrease of h^1. In addition, when h^1 is fixed, with the increase of the attack probability α, the maximum value of h^2 is smaller. Table 2 provides the maximum value of h^2 for different β_1 when h^1 and α are fixed. It is easy to see from table 2 that the maximum value of h^2 becomes smaller gradually with the decrease of β_1.

Specify the values of the parameters in theorem 2 as $\alpha = 0.4$, $\delta = 0.1$, $\beta_1 = 0.6$, $h^1 = 0.1$, $h^2 = 0.2$, $\lambda = 0.3$. The solution that satisfy the LMIs (23) of matrix K is solved via MATLAB LMI Toolbox as:

$$K = \begin{bmatrix} 1.3210 & -0.0272 \\ 0.0821 & 0.0510 \end{bmatrix}.$$

By using the parameters mentioned above, the time response of the error system state $r(t)$ and the transmitted data $\varepsilon(t)$, the control input and the FDIA signal $g(x(t))$ with occurrence probability $\alpha(t)$ are demonstrated in figure 2. From figure 2(a), we can see that system (1) can reach exponentially synchronized by the SSDC (2), which demonstrates the effectiveness of the designed controller in mitigating the FDIAs.

5. Conclusions

The security control of master-slave MJNNs has been investigated via SSDC and LLF subject to FDIAs in this paper. SSDC can not only solve the problem of data redundancy, but also mitigate the impact of FDIAs on the system performance. An error system model is established with multi input-delays. Then, a $\beta_j(t)$-dependent LLF is constructed to reduce the conservativeness of the synchronization condition (i.e. theorem 1). On this basis, an easy-to-solve design algorithm for SSDC is given (i.e. theorem 2). Finally, through a numerical example, it is verified that SSDC can realize the exponential synchronization of MJNNs under FDIAs, and this SSDC synchronization method has been applied to image encryption and decryption successfully.

ORCID iDs

Xia Huang https://orcid.org/0000-0002-4955-8318
Min Xiao https://orcid.org/0000-0002-8992-153X

References

[1] Yang X, Song Q, Cao J and Lu J 2019 Synchronization of coupled Markovian reaction-diffusion neural networks with proportional delays via quantized control *IEEE Trans. Neural Netw. Learn. Syst.* **30** 951–8
[2] Wang B and Zhu Q X 2020 Stability analysis of discrete time semi-Markov jump linear systems *IEEE Trans. Autom. Control* **65** 5415–21
[3] Man J, Zeng Z, Xiao Q and Zhang H 2022 Exponential stabilization of semi-Markov reaction-diffusion memristive NNs via event-based spatially pointwise-piecewise switching control *IEEE Trans. Neural Netw. Learn. Syst.* (https://doi.org/10.1109/TNNLS.2022.3190694)
[4] Huang X, Zhou Y, Kong Q, Zhou J and Fang M 2020 $H\infty$ synchronization of chaotic Hopfield networks with time-varying delay: a resilient DOF control approach *Commun. Theor. Phys.* **72** 015003
[5] Yao Z, Zhang Z, Wang Z, Lin C and Chen J 2022 Polynomial synchronization of complex-valued inertial neural networks with multi-proportional delays *Commun. Theor. Phys.* **74** 125801
[6] Tang R, Su H, Zou Y and Yang X 2022 Finite-time synchronization of Markovian coupled neural networks with delays via intermittent quantized control: linear programming approach *IEEE Trans. Neural Netw. Learn. Syst.* **33** 5268–78
[7] Zhu Q X and Cao J D 2012 Stability analysis of Markovian jump stochastic BAM neural networks with impulse control and mixed time delays *IEEE Trans. Neural Netw. Learn. Syst.* **23** 467–79
[8] Shen H, Hu X, Wang J, Cao J and Qian W 2023 Non-fragile $H\infty$ synchronization for Markov jump singularly perturbed

coupled neural networks subject to double-layer switching regulation *IEEE Trans. Neural Netw. Learn. Syst.* **34** 2682–92

[9] Shu J, Wu B and Xiong L 2022 Stochastic stability criteria and event-triggered control of delayed Markovian jump quaternion-valued neural networks *Appl. Math. Comput.* **420** 126904

[10] Song X, Zhang R, Ahn C K and Song S 2022 Synchronization for semi-Markovian jumping reaction-diffusion complex dynamical networks: a space-time sampled-data control scheme *IEEE Trans. Netw. Sci. Eng.* **9** 2684–96

[11] Fridman E 2010 A refined input delay approach to sampled-data control *Automatica* **46** 421–7

[12] Yang X T and Zhu Q X 2021 Stabilization of stochastic retarded systems based on sampled-data feedback control *IEEE Trans. Syst., Man. Cybern., Syst.* **51** 5895–904

[13] Yang X, Liu Y, Cao J and Rutkowski L 2020 Synchronization of coupled time-delay neural networks with mode-dependent average dwell time switching *IEEE Trans. Neural Netw. Learn. Syst.* **31** 5483–96

[14] Tao B, Xiao M, Zheng W, Zhou Y, Ding J, Jiang G and Wu X 2023 Design and dynamics analysis of a time-delay feedback controller with distributed characteristic *IEEE Trans. Autom. Control* **68** 1926–33

[15] Zhang Q, Liu K, Pang Z, Xia Y and Liu T 2022 Reachability analysis of cyber-physical systems under stealthy attacks *IEEE T. Cybern.* **52** 4926–34

[16] Xu Z, Tang R, Sun Y, Li X and Yang X 2022 Secure synchronization of coupled systems via double event-triggering mechanisms with actuator fault *IEEE Trans. Netw. Sci. Eng.* **9** 3580–9

[17] Zhou C, Hu B, Shi Y, Tian Y C, Li X and Zhao Y 2021 A unified architectural approach for cyberattack-resilient industrial control systems *Proc. IEEE* **109** 517–41

[18] Wang H, Yang X, Xiang Z, Tang R and Ning Q Synchronization of switched neural networks via attacked mode-dependent event-triggered control and its application in image encryption *IEEE T. Cybern.* (https://doi.org/10.1109/TCYB.2022.3227021)

[19] Yao L, Huang X, Wang Z and Liu K 2023 Secure control of Markovian jumping systems under deception attacks: an attack-probability-dependent adaptive event-trigger mechanism *IEEE Trans. Control Netw. Syst.* (https://doi.org/10.1109/TCNS.2023.3269007)

[20] Yao L and Huang X 2023 Memory-based adaptive event-triggered secure control of Markovian jumping neural networks suffering from deception attacks *Sci. China Technol. Sci.* **66** 468–80

[21] Zhang Q, Liu K, Han D, Su G and Xia Y 2023 Design of stealthy deception attacks with partial system knowledge *IEEE Trans. Autom. Control* **68** 1069–76

[22] Zhang X M, Han Q L, Ge X and Ding L 2020 Resilient control design based on a sampled-data model for a class of networked control systems under denial-of-service attacks *IEEE T. Cybern.* **50** 3616–26

[23] Hu L, Wang Z, Han Q L and Liu X 2018 State estimation under false data injection attacks: security analysis and system protection *Automatica* **87** 176–83

[24] Wang X and Ma Y 2023 Adaptive non-fragile sliding mode control for switched semi-Markov jump system with time-delay and attack via reduced-order method *Appl. Math. Comput.* **440** 127670

[25] Zhao J and Yang G 2023 Fuzzy adaptive secure tracking control against unknown false data injection attacks for uncertain nonlinear systems with input quantization *Appl. Math. Comput.* **437** 127551

[26] Gao H J, Wu J L and Shi P 2009 Robust sampled-data $H\infty$ control with stochastic sampling *Automatica* **45** 1729–36

[27] Briat C 2016 Stability analysis and stabilization of stochastic linear impulsive, switched and sampled-data systems under dwell-time constraints *Automatica* **74** 279–87

[28] Zhang R M, Zeng D Q and Zhong S M 2018 New approach on designing stochastic sampled-data controller for exponential synchronization of chaotic Lur'e systems *Nonlinear Anal: Hybrid Syst.* **29** 303–21

[29] Wu Z G, Shi P, Su H Y and Chu J 2013 Sampled-data synchronization of chaotic Lur'e systems with time delays *IEEE Trans. Neural Netw. Learn. Syst.* **24** 410–21

[30] Zeng H B, Teo K L and He Y 2017 A new looped-functional for stability analysis of sampled-data systems *Automatica* **82** 328–31

[31] Chen W H, Chen J L and Zheng W X 2020 Delay-dependent stability and hybrid $L_2 \times l_2$-gain analysis of linear impulsive time-delay systems: a continuous timer-dependent Lyapunov-like functional approach *Automatica* **120** 109119

[32] Zeng H B, Zhai Z L, He Y, Teo K L and Wang W 2020 New insights on stability of sampled-data systems with time-delay *Appl. Math. Comput.* **374** 125041

[33] Ali M S and Saravanakumar R 2014 Improved delay-dependent robust $H\infty$ control of an uncertain stochastic system with interval time-varying and distributed delays *Chin. Phys.* B **23** 120201

[34] Yuan Y, Song Q, Liu Y and Alsaadi F E 2019 Synchronization of complex-valued neural networks with mixed two additive time-varying delays *Neurocomputing* **332** 149–58

[35] Masjed-Jamei M 2009 A functional generalization of the Cauchy–Schwarz inequality and some subclasses *Appl. Math. Lett.* **20** 1335–9

[36] Yao L, Wang Z, Huang X, Li Y, Ma Q and Shen H 2023 Stochastic sampled-data exponential synchronization of Markovian jump neural networks with time-varying delays *IEEE Trans. Neural Netw. Learn. Syst.* **34** 909–20